

## Research Article

<https://doi.org/10.1631/jzus.A2100188>



# A new technique for high-fidelity cutting technology for hydrate samples

Hai ZHU<sup>1</sup>, Jia-wang CHEN<sup>1,3✉</sup>, Zi-qiang REN<sup>1</sup>, Pei-hao ZHANG<sup>1</sup>, Qiao-ling GAO<sup>1</sup>, Xiao-ling LE<sup>1</sup>, Chun-ying XU<sup>2</sup>, Kai HE<sup>1</sup>, Peng ZHOU<sup>1</sup>, Feng GAO<sup>1</sup>, Yu-ping FANG<sup>1</sup>

<sup>1</sup>Institute of Ocean Engineering and Technology, Ocean College, Zhejiang University, Zhoushan 316021, China

<sup>2</sup>Key Lab of Digital Signal and Image Processing of Guangdong Province, School of Engineering, Shantou University, Shantou 515063, China

<sup>3</sup>Southern Marine Science and Engineering Guangdong Laboratory (Guangzhou), Guangzhou 511458, China

**Abstract:** Designing a high-fidelity cutting device is one of the difficulties in hydrate samples pressure-holding transfer. Due to the limitations of the existing mechanical system, there is much damage to the cut surface of hydrate samples, with many chips produced, which seriously affects the quality of samples. In this paper, a new cutting device utilizes two servo motors to achieve a high degree of automation. Using the Archimedes spiral, it achieves low disturbance of the cut surface and provides accurate control of the process. In addition, due to the operation of the sample long-stroke push unit, cutting hydrate samples of any length with almost no chips within a short cutting time can be achieved. Laboratory and sea tests have achieved all design requirements of the equipment and strongly demonstrate its benefit and stability. It is concluded that this new high-fidelity cutting technology is practically efficient. The physical state of the hydrate can be maintained to the greatest extent, and thus the new equipment provides significant support for the exploration and development of hydrate resources.

**Key words:** High-fidelity; Cutting technology; Hydrate samples; Automation

## 1 Introduction

Subsea sampling can accelerate the efficiency and accuracy of the exploration and geological surveys of marine resources. It can save costs, and provide good social and economic benefits (Zhao et al., 2017; Yoneda et al., 2019). Taking natural gas hydrates as an example, sampling a natural gas hydrate to obtain relevant parameters can provide theoretical support for its commercial exploitation (Li et al., 2018; Ye et al., 2018, 2020). Drilling for samples is a conventional technique in marine resource exploration and geological investigation (Tsuchiya et al., 2019; Hoang et al., 2021). After the hydrate has been sampled, the sampler is transported to a ship. The sample tube is removed from the sampler and is sent to the pressure maintaining transfer device for pressure transfer, test analysis,

cutting, and storage. High-fidelity samplers are an established instrument for marine researchers because of their ability to maintain the characteristics and composition of samples (Parkes et al., 2009; Moore et al., 2020; Wang et al., 2020). The hydrate in the samplers would decompose with the decrease of external pressure and increase of temperature before it reaches sea level (Hyodo et al., 2014), if there were no pressure maintenance mechanism, the resulting gas expanding inside the hydrate would destroy its original structure (Dai and Santamarina, 2014). Therefore, maintaining the original pressure and temperature at the sampling point is very important for hydrate research (Zhang et al., 2019). It should be noted that getting high-fidelity hydrate samples to the workboat deck is not all that needs to be done before laboratory analysis (Gao et al., 2020). The samplers are not suitable for long-term core storage, and a sample storage tank is the best core storage choice. Therefore, the process from the samplers to the storage chamber (including cutting) must ensure that any fluctuation in the storage environment parameters of the hydrate samples does not cause structural and state changes in them.

✉ Jia-wang CHEN, arwang@zju.edu.cn

✉ Hai ZHU, <https://orcid.org/0000-0002-4681-163X>  
✉ Jia-wang CHEN, <https://orcid.org/0000-0002-6351-0062>

Received Apr. 20, 2021; Revision accepted July 12, 2021;  
Crosschecked Dec. 2, 2021

© Zhejiang University Press 2022

On the one hand, the samplers usually need to follow the design principle of making the obtained sample have the highest research value (in general, the longer the sampling tube, the higher the research value); but on the other hand, the size of the sample tube is not compatible with most laboratory analytical instruments, such as computed tomography (CT) scanners. The solution is to cut the hydrate sampling tube into segments of the required size, transfer them to the sample storage tank, and finally place the sample storage tank in the laboratory analytical instrument. Core sample processing needs to be completed before laboratory analysis, and for that high-fidelity cutting technology of the hydrate sample is an essential component in many processing steps and an essential guarantee of sample quality (Gao et al., 2020).

At present, there is a mature and commercially available comprehensive pressure protection test system (pressure core analysis and transfer system (PCATS)) (Priest et al., 2015), which has a wide range of functions, including long-stroke push, pressure-holding cutting, temperature control system, secondary sampling, and non-destructive measurement. In the cutting unit alone, PCATS first uses a rotating cutter to cut the plastic casing and then uses a reciprocating saw cutter to cut the sediment core. However, the system has many disadvantages, such as manual control, frequent loading and unloading for multiple cuts, and difficulty of precision control. The cutting environment of the hydrate sample tubes is a confined space at high pressure and low temperature (Zhu et al., 2018), which brings significant difficulties for power transmission, cutting process control, and core debris cleaning.

Given the shortcomings of PCATS, our team has developed a new set of core pressure-maintaining

transfer devices. The hydrate core sample tube is 2 m long and 48.5 mm in diameter. The sample tube is made of polyvinyl chloride (PVC) and contains a whole section of hydrate. The length of the whole pressure retaining transfer system is 18 m, and the outer diameter varies according to the function of each part, but the inner diameter is basically 50 mm. Its structure is shown in Fig. 1.

Combining a pressure and temperature maintaining unit and a long-stroke push unit, a pressure-holding transfer system for the hydrate samples is formed. The pressure and temperature maintaining unit is responsible for the temperature and pressure regulation of the entire pressure-holding transfer system for the hydrate samples, and controls the heat exchange using compressors, reservoirs, evaporators, condensers, and expansion valves, with an accuracy of 0.5 °C (Zhang et al., 2019). A stable external environment (the same temperature and pressure as the sampling point) is provided for the high-fidelity cutting device. The long-stroke push unit is responsible for the movement and precise positioning of the sample tube within the pressure-holding transfer system. In conjunction with the high-fidelity cutting unit, the sample tube can be cut to almost any length (Ren et al., 2020). With these two units, both the long-term stability of temperature and pressure and the smooth long-stroke transfer of sampling tubes can be achieved.

## 2 Mechanical structure design

### 2.1 Overall design of the high-fidelity cutting device

Under 30 MPa pressure and 2–4 °C temperature conditions, the cutting device should cut the hydrate

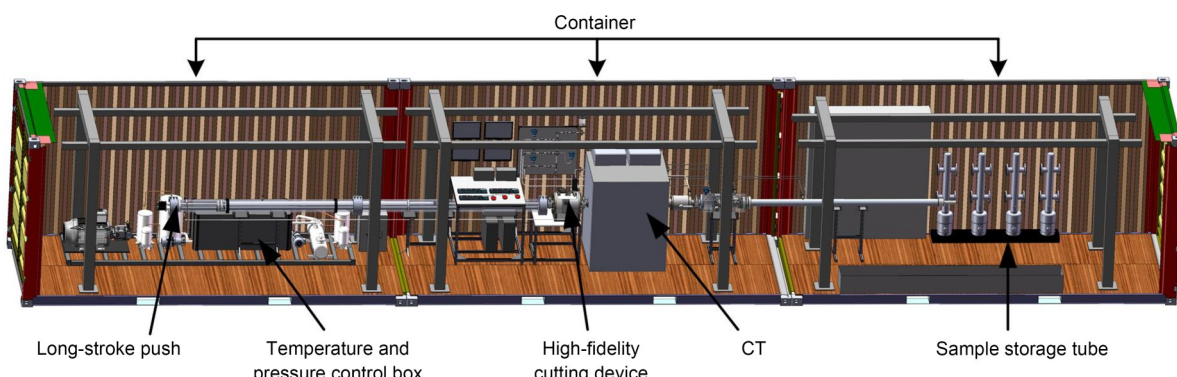
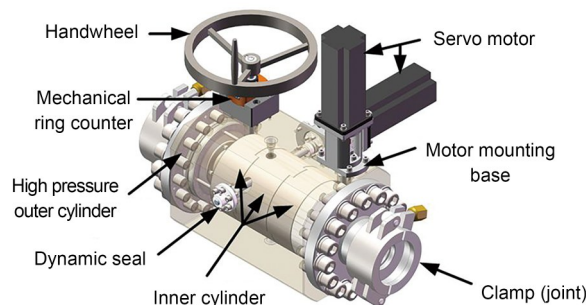


Fig. 1 Overall pressure maintaining transfer device

sample tubes smoothly and quickly without interference. Common pipe cutting methods are not carried out in pressurized enclosed spaces, so the restriction on radial dimensions is relatively weak, and the cutting environment is not filled with water. Cutting methods available include grinding wheel cutting, electrical spark cutting, and high-pressure water cutting (Toussaint, 2008; Hayashi et al., 2014). However, these methods are not applicable due to the particulars of the working environment and the unstable nature of the hydrates. The problems to be solved in high-fidelity cutting technology include temperature and pressure fluctuation, the disturbance of cutting to the sample, dynamic sealing of moving parts, control of the cutting process, and compatibility of cutting objects. An illustration of the high-fidelity cutting device is shown in Fig. 2, and the design parameters for the equipment are:

- (1) Working pressure: 30 MPa;
- (2) Operating temperature: 2–4 °C;
- (3) Pressure and temperature fluctuation during transfer:  $\leq 10\%$ ;
- (4) Single cutting time:  $\leq 3$  min;
- (5) No sample contamination from cutting operations;
- (6) Controllable cutting process and calculable cutter position.



**Fig. 2** High-fidelity cutting device

To achieve less sample disturbance than in PCATS, full-range rotary cutting is used instead of reciprocating cutting and servo motors are used instead of handwheels to achieve better cutting process control. In addition, an independent anti-blocking structure is designed to solve the problems of frequent loading and unloading. The high-fidelity cutting device in the sampling tube includes a clamping mechanism and a cutting mechanism. The connection between the high-fidelity cutting device and other parts of the hydrate samples pressure-holding transfer system is designed in a quick-connect form to facilitate offshore operations and therefore clamps and end-cap flanges are included at both ends of the device. Also, two servo motors are used to drive the cutting mechanism, and a handwheel is used to drive the clamping mechanism. To achieve a high-pressure dynamic seal, and in consideration of the ease of assembly of the remaining parts, some auxiliary parts are designed. The parameters of the high-fidelity cutting device are shown in Table 1.

## 2.2 Internal structure composition

The high-fidelity cutting device performs two functions, clamping and cutting, which are realized by two mechanisms with the same principle but slightly different structures. Two servo motors control the cutting and a handwheel controls the clamping. An electronic control system matched with the cutting operation is designed separately and is mainly used to control the rotation direction and speed of the servo motors. Details will be given later in this paper. Besides, the adoption of an Archimedes spiral makes it possible to control the circumferential rotation speed and radial feed speed of the cutter accurately. The electronic control system realizes start-stop, emergency braking, and automatic reset of the cutting. It is also used to calculate the knife position in real-time. The

**Table 1** Parameters of the high-fidelity cutting device

Parameter	Description
Total length of high-fidelity cutting device, $L$ (mm)	618
Total width of high-fidelity cutting device, $M$ (mm)	548
Total height of high-fidelity cutting device, $H$ (mm)	518
Main materials of other parts	17-4PH
Alternating current (AC) servo motor model	DEL ECMA-J10807SS
High performance motion control type AC servo drive	DELTA ASD-A2-0743-M
Power of high-fidelity cutting device, $P$ (W)	1500
Input voltage, $U$ (V)	380

low chip and anti-blocking design make possible multiple cuts without removing the knife. The cutting device section is shown in Fig. 3.

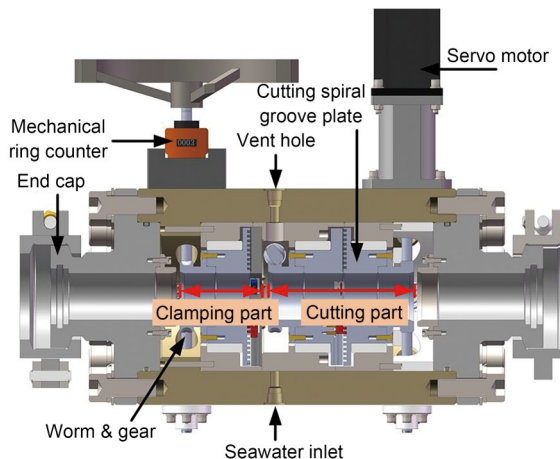


**Fig. 3** Cutting device section

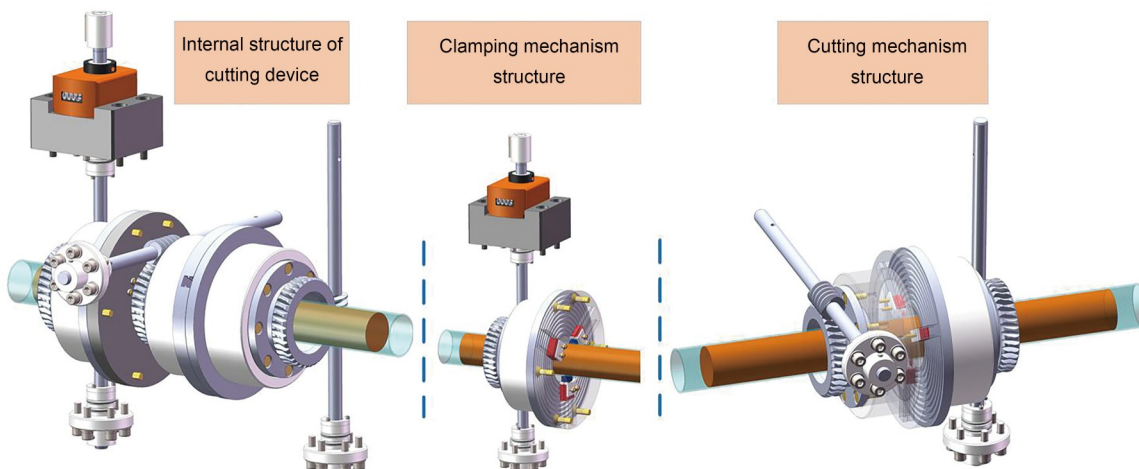
The sample tube is very fragile as the wall thickness is only 1.5 mm (Yi et al., 2017; Gao et al., 2020). To prevent the sample tube from breaking, the clamping mechanism must not exert too much force. Although a servomotor and sensor design would be more automated, it would complicate the structure, and additional control programs would be required, increasing the uncertainty. Because the required clamping accuracy is not high, the movement of the clamping mechanism can be quickly and conveniently controlled by installing a handwheel on the transmission worm.

Fig. 4 is the high-fidelity cutting device's primary working mechanism for clamping and cutting.

As can be seen from the clamping mechanism components, the clamping part consists of a clamping jaw limit plate fixed with countersunk bolts and a slotted plate with helical lines. The clamping jaws are fixed between the two. Rotating the handwheel drives the worm wheel to rotate, thereby driving the clamping spiral groove disk to rotate, and the clamping jaws are fed or retracted accordingly. The mechanical counter installed on the clamping device provides a reference for the degree of clamping. The clamping jaw head is designed as a toothed shape for better fixing the thin-walled sampling tube. The experiment also shows that the clamping effect can achieve the preset effect without slippage. The most significant difference between the cutting mechanism and the clamping mechanism is that the former has an additional drive input. The worm gear and worm parameters of cutting mechanism are shown in Table 2.

### 2.3 Quality section guarantee method

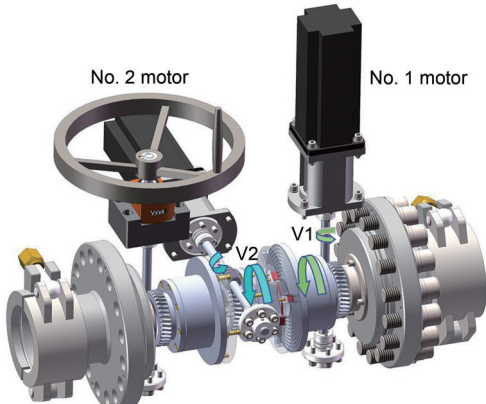
The two pairs of worm gears connect the cutting limit plate and the cutting spiral groove plate respectively. They rotate in the same direction but at different speeds. The speed of the cutter limit disc (V1) determines the circumferential rotation speed, and the speed difference between the plates determines the feed and return speed of cutting. For example, if the cutter head speed V1 (anti-clockwise) is greater than V2 (clockwise), the tool will feed; if the cutter head speed V1 (anti-clockwise) is less than V2 (clockwise), the cutter will retract. The rotation direction of V1 and V2 above is the same as shown in Fig. 5.



**Fig. 4** Schematic realization of the high-fidelity cutting device

**Table 2 Worm gear and worm parameters of cutting mechanism**

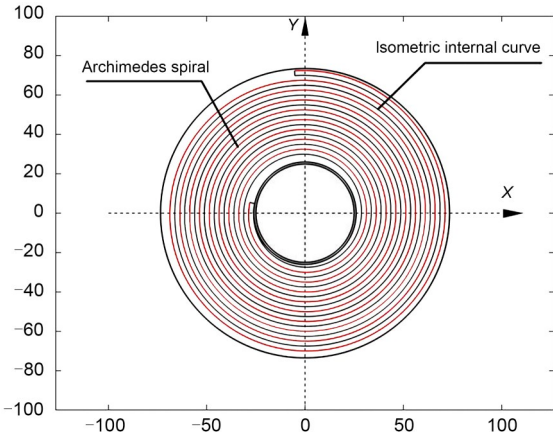
Parameter	Description	
	Worm gear	Worm
Axial modules, $m_n$	2	2
Number of worm teeth or heads, $z$	36	2
Tooth angle (°)	20	20
Coefficient of addendum height	1	1
Axial modulus, $\gamma$ (°)	12.53	12.53
Rotation direction	Right	Right
Radial displacement coefficient, $x_n$	0	0
Transmission ratio, $i$	18	18
Transmission center distance (mm)	45	45

**Fig. 5 Direction of rotation**

As shown in Fig. 6, the key to ensure the quality of the cutting surface lies in application of an Archimedes spiral in this cutting equipment. The Archimedes spiral is an iso-velocity ratio spiral because it advances an equal distance with each rotation cycle. This feature ensures a constant feed speed and high quality of the core sample cut surface due to the circumferential rotation of the cutter (Kamruzzaman and Dhar, 2009; Saelzer et al., 2020; Zhu et al., 2020). The Archimedean spiral is determined by the following parametric equation:

$$\begin{cases} x = \frac{p\cos(\theta)}{\pi} + \frac{p\theta\sin(\theta)}{\pi}, \\ y = \frac{p\sin(\theta)}{\pi} - \frac{p\theta\cos(\theta)}{\pi}, \end{cases} \quad (1)$$

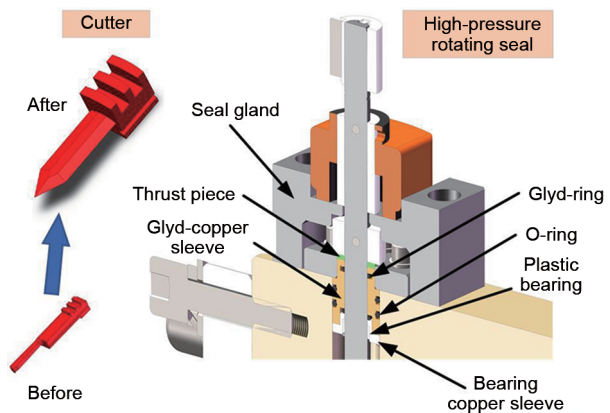
where  $p$  represents the corresponding increase in the polar diameter of the Archimedes spiral for each revolution, and its value in this equipment is 2.5 mm.  $\theta$  represents the polar angle of Archimedes spiral.

**Fig. 6 Surface curve of spiral grooved plate (unit: mm)**

The isometric internal curve is 1.25 mm apart from the Archimedes spiral. According to the different usages of clamping the spiral groove plate and cutting the spiral groove plate, the parameter equation interval of the Archimedes spiral is set as  $[12.39\pi, 26.55\pi]$  and  $[11.43\pi, 29.02\pi]$ .

#### 2.4 Realization of high-pressure dynamic seal and anti-silting design of the cutter

The structure of the high-pressure rotating seal is shown in Fig. 7. The sealing structure includes Glyd-ring, O-ring, plastic bearing, bearing copper sleeve, Glyd-copper sleeve, thrust piece, and seal gland. The thrust piece eliminates the lateral force of the worm. Because of the imbalance of internal and external pressures, the high internal pressure will eject the Glyd-copper sleeve of the bearing outwards, so a seal gland is used for corresponding low dissipation. The dynamic seal of the worm is achieved using plastic

**Fig. 7 High-pressure dynamic seal and cutter improvement device**

bearings and Glyd-rings, while the O-rings guarantee the static seal. The dimensions of the above seals are determined in accordance with the design manual, and the design calculations are carried out.

Tools are an essential basis for cutting, so their structural design is extremely important. We have made several trial cuts and accordingly have made several improvements that have resulted in almost disturbance-free and chip-free cutting. The cutting tool is designed with reference to the lathe tool, but due to the low strength of the thin-walled plastic pipe, the sample tube will shake around the center axis of the cylinder in the case of a long cantilever (Zhu et al., 2020). Therefore, the end of the cutter needs to be designed in a spire style, which facilitates the cutter fitting into the sample tube (Yi et al., 2017; Lukin et al., 2020). The cutting surface needs to be as smooth as possible, so the thickness of the cutting knife needs to be minimized. In order to reduce shaking during cutting, the edge of the cutting knife should be sharp. The expected cutting effect can be achieved by installing such a cutter on the lathe turret but, during assembly, the cutter cannot rotate flexibly in the grooved plate, so we increased the tolerance and achieved a smooth rotation of the cutter in the grooved plate.

Considering that the current cutting device adopts the combination of spiral groove plates and limit plates, there is a large gap between them, and chips will inevitably occur during cutting (Zhu et al., 2018). The presence of small stones and sludge in the sample makes it possible for impurities to enter the gap, leading to the tool's rotary blockage. A set of anti-silting structures is designed separately based on spiral groove plates to prevent silt and small stones from entering the spiral groove plates and affecting cutting (Pang et al., 2019). The anti-blockage design mainly involves two kinds of cutters: cutter and clamping jaw. A similar anti-blockage principle is adopted to modify the equipment according to the shape of the cutters. A closed ring face is formed by using the boss of the limit plates and the spiral groove plates. Also, due to the movement of the cutters, a gap in the stroke is formed, and the anti-siltation of this gap is achieved by using a plug. For plug installation, slots, threaded mounting holes, and cutter holes are designed on the plug. Since the sampling tube needs to be moved in the pressure-retaining cutting device, the plug is designed as a curved surface. Besides, to avoid the tool rushing

through the plug and pushing the plug out, stroke determination is required for the spiral grooved plates. The anti-blocking design is shown in Fig. 8.

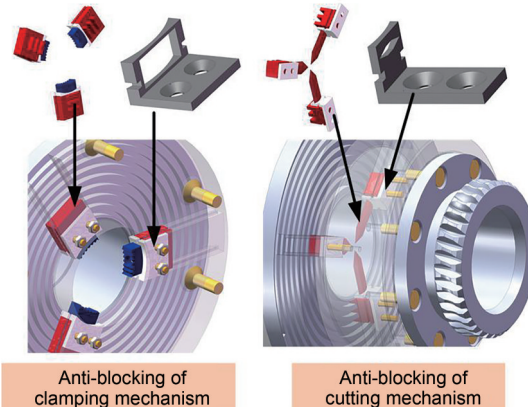


Fig. 8 Anti-blocking design

### 3 Electronic control design

The pressure-holding transfer system's control system for the hydrate samples includes the upper machine monitoring software, deck high-voltage power supply, central control system board, power conversion module, motor control system, temperature/pressure sensor, and other parts. The overall composition of the control system is shown in Fig. 9.

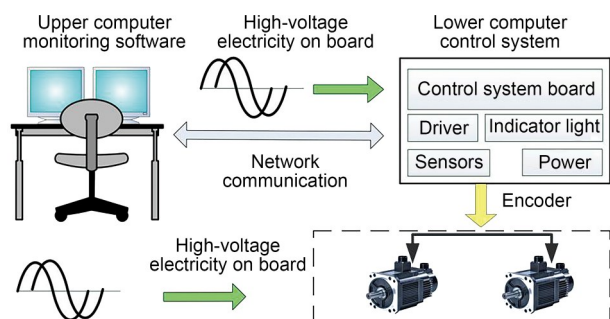


Fig. 9 Overall composition of the control system

The shipboard 440-V alternating current (AC) is converted to 380-V AC and 220-V AC through the distribution cabinet and then to direct current (DC) with different voltages. The above power supply is used to supply the motor, temperature and pressure maintenance unit, control system boards, relay, and chips. Communication data between the control board and the upper computer is transmitted via the network

interface and twisted-pair wire, and the control board controls the motor driver through the CANopen protocol to control the operation of the motors. The control panel gathers the collected data, such as motor speed and torque, and sends them to the upper computer by a communication protocol. They are displayed on the monitoring screen as a dial or curve drawn by the upper computer. The control commands of the motor and the commands to switch on and off the valves sent by the upper computer will also be sent to the control board through the communication protocol. The control board controls all parts to perform corresponding actions to complete the upper computer's instructions.

As shown in Fig. 10, the hardware composition of the industrial computer mainly includes an AC-DC power supply system, control board system circuit, and motor driver. As shown in Fig. 10, the AC-DC power supply system converts 380-V AC input to 220-V AC, then 220-V AC to 24-V DC for power supply of the control system board, valves, and lights. Also, 24-V DC is converted to 12-V DC and 3.3-V DC for current supply to relays, operational amplifier chips, central processing unit (CPU) chips, and fans. In the control board system, besides the CPU's primary circuit, a network hardware circuit is also included to achieve network communication with the host computer. The current/voltage (I/V) conversion circuit converts the 4–20 mA current signal sent by the sensor into a 1–5 V voltage signal. The analog to digital (AD) acquisition circuit reads the converted voltage signal and fits it into the intuitive temperature and pressure display. In addition, the CPU controls the switching

on and off of relay groups through input/output (I/O), which further controls various external devices. The motor driver occupies most of the space of the whole industrial control cabinet. By setting the motor driver as a controller area network (CAN) interface of each node and control system, CANopen local area network (LAN) is formed to control the motor. Two drivers are used to control the two motors throughout the transfer system for cutting the core pipe.

As the window to the whole system, the upper computer software is important for human-machine interaction. The development language of the upper computer control software designed in this system is C#, the development environment is in .NET Framework 4.5, and the development software is Visual Studio 2019. The system's software program is based on Windows Forms, and the main application model is in .NET Framework, with a wide range of graphical desktop applications that are easy to update and deploy. The software program consists of two parts: the first part is the control provided by the platform, dragging it to the specified position of the window, changing the color, size, format, and other data in its attributes as needed, and the system background will automatically generate the corresponding underlying program code; the second part is based on the data protocol uploaded by the control board and the control commands issued by the host computer. The logical classification is completed by analyzing, cutting, and dividing the data, and is dynamically combined with the controls of the first part to form a complete run for the program. The interface layout is completed as shown in Fig. 11.

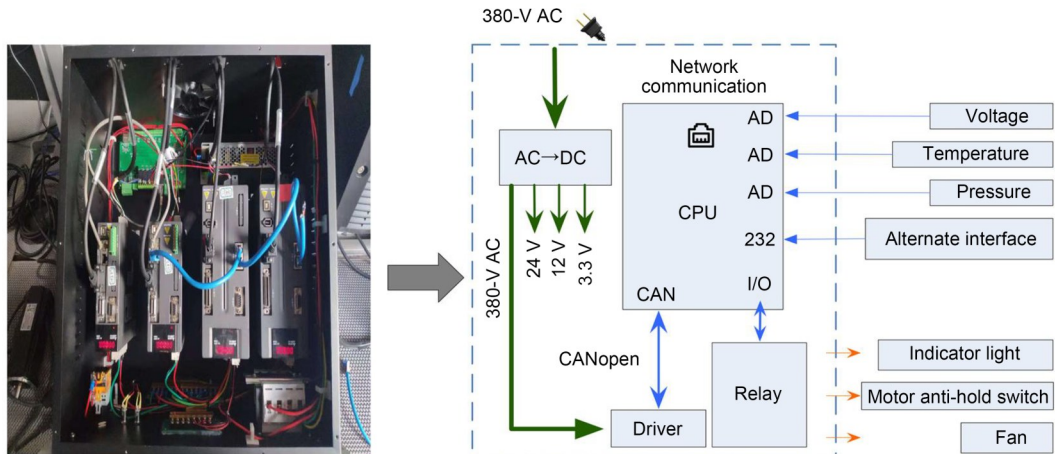


Fig. 10 Hardware composition of industrial computer



Fig. 11 Upper computer interface

The cutting-related parts on the upper computer interface include the following:

1. Dynamic display region for sample handling: this dynamically displays the core sample tube position and provides position information for sample tube cutting.
2. Cutting motors' status display region: this region dynamically displays the speed and torque of the cutting motor on a dial.
3. Cutting control buttons: these regulate the core cutting process in the core tube by multiple control buttons for automatic control.
4. Indicator light region: this displays the running status of the cutting motor, open or closed.
5. Log region: this displays the log preparation of network connection, with a text warning in case of a program operation error.

The internal logic of the whole interface layout includes the reading and clipping of the uploaded data and the dynamic association of the distributed data. The logical process of uploading data involves sending data using a network protocol, judging the frame head and frame tail after receiving, obtaining the data information, saving the data information in the log, and then cutting the data information to display it in each display area. The logic flow of uploading data involves a motor control command input through the cutting control area and other positions and is then sent to the control board of the lower computer through the network interface after splicing. A check code is added, and the data sent can also be saved in the log.

## 4 Calculations

### 4.1 Pressure maintaining calculations

Because the internal pressure of the high-fidelity cutting device is up to 30 MPa, the size of the outer barrel involves a choice of the bore diameter, overall length, wall thickness, and material. The sample tube's outer diameter determines the depth of feed required by the tool and the maximum depth of feed for the tool. The outer diameter of the sample tube can roughly determine the bore diameter of the outer cylinder. The corresponding wall thickness is calculated based on the bore diameter, taking into account a safety factor.

It is noted that the wall thickness of the high-pressure outer cylinder should be designed to resist the working environment pressure of 30 MPa, and the wall thickness is calculated by

$$\delta = \frac{P_c D_i}{2[\sigma]^t \phi - P_c}, \quad (2)$$

where  $P_c$  is the ambient pressure during equipment operation,  $D_i$  is the inner diameter of the high-pressure outer cylinder,  $[\sigma]^t$  is the allowable stress of materials at design temperature  $t$ , and  $\phi$  is the welding coefficient.

Intensity examination was carried out by the following formula:

$$\frac{P_T (D_i + \delta_e)}{2\delta_e} \leq 0.9\phi R_{eL}, \quad (3)$$

where  $P_T$  is the test pressure,  $\delta_c$  is the effective thickness of the high-pressure outer cylinder, and  $R_{cl}$  is the yield strength of its material.

Similar calculations were carried out during the design of the device. The pressure-bearing body of the high-fidelity cutting device is the high-pressure outer cylinder. Aluminum alloy 7075 was chosen, taking into account corrosion resistance, strength, and price. Its parameters are shown in Table 3.

**Table 3 Parameters of the high-pressure outer cylinder**

Parameter	Description
Length, $l$ (mm)	550
Inner diameter, $d$ (mm)	160
Side length (mm)	232
Material	7075T6
Density, $\rho$ (kg/m <sup>3</sup> )	$2.81 \times 10^3$
Tensile strength, $\sigma_t$ (Pa)	$5.72 \times 10^8$
Young's modulus, $E$ (Pa)	$7.17 \times 10^{10}$
Poisson's ratio, $\nu$	0.33

#### 4.2 Force analysis of the cutters

Force analysis of the cutting knife is carried out according to the curve characteristics of the Archimedes spiral, and the power required for cutting can be calculated, providing a reference for motor selection. Fig. 12 shows the force analysis of a cutting knife (Li and

Kishawy, 2006).  $F_p$  is the friction force on the cutting spiral grooved plate due to the rotation of the cutters;  $F_{pr}$  and  $F_{pt}$  are the radial and tangential components of  $F_p$ , respectively;  $P$  is the positive pressure of cutter on cutting spiral groove plate;  $P_r$  and  $P_t$  are the radial and tangential components of  $P$ , respectively;  $P'_t$  is the reaction force of  $P_t$ ;  $P'_r$  is the reaction force of  $P_r$ ;  $F_t$  and  $F_n$  are the radial and tangential components of cutting force, respectively.

$$\sum F_x = fp \cos\theta \cos\theta + p \sin\theta + p \cos\left(\frac{\pi}{6} + \theta\right) - fp \cos\theta \cos\left(\frac{\pi}{3} - \theta\right) - p \cos\left(\frac{\pi}{6} - \theta\right) - fp \cos\theta \cos\left(\frac{\pi}{3} + \theta\right) = 0, \quad (4)$$

$$\sum M_o = T - T_f - 3P_t h - 3F_{pt} h = 0, \quad (5)$$

$$P = \frac{T - T_f}{3h(\sin\theta + f\cos\theta)}, \quad (6)$$

$$P_r = \frac{T - T_f}{3h(\tan\theta + f)}. \quad (7)$$

In the upper model,  $h$  is the radius of action of the plate wire plane thread,  $f$  is the friction coefficient of the contact surface part,  $F_x$  is the force in the  $X$  direction of the coordinate axis,  $M_o$  represents the

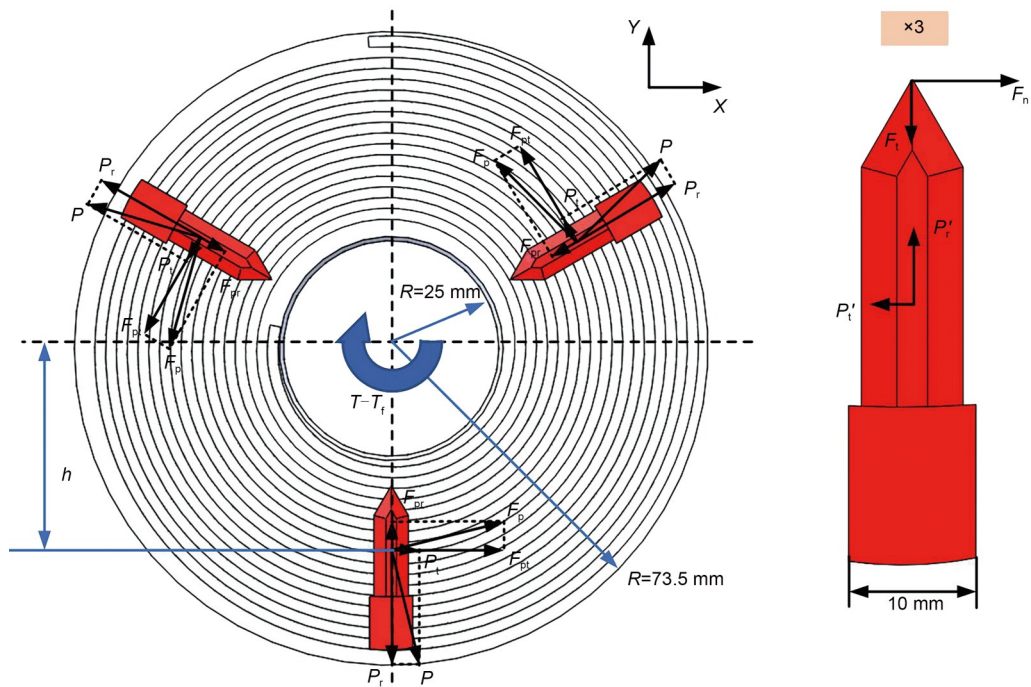


**Fig. 12 Force analysis of cutters**

torque force on the cutting spiral grooved plate,  $T$  is the driving torque, and  $T_f$  is the obstruction of the friction moment. By combining the equations, the torque required by the motor can be obtained. The servo motors are selected according to the torque, and other factors (such as control method, power supply voltage, and rated power) that are required.

#### 4.3 Cutting process simulation

Simulation is a standard analysis method. In the process of high-fidelity cutting design, ABAQUS software is used for simulation. On the one hand, the simulation analysis of the cutter cutting process provides the design basis; on the other hand, it also proves the rationality of the design (Yen et al., 2004; Attanasio et al., 2010).

According to the design, a single cut takes 2 min, so the process of a single feed is simulated. The simulation result of a single cutting is shown in Fig. 13. Simplified cutters are used in the simulation, and the number is changed to 4 to achieve symmetrical cutter distribution and to speed-up the calculation. The simulation results show that the cutter can penetrate the hydrate sample wholly and smoothly. It can be concluded from the stress-strain diagram that there is a maximum stress at the tool-tip. With the penetration of the cutting knife, the disturbance to the hydrate in the sample tube increases gradually until the peak of the disturbance (about 105 s) is reached. After cutting, the influence of the tool will fall back to a lower level.

The cutter rotates clockwise, and the stress distribution on the tangential plane also rotates in the direction of the cutter movement. Since the sample tube's material is PVC and the strength of hydrate is obviously lower than that of PVC, it is difficult to simulate by setting all the cutting tools to PVC. The disadvantage of this is that it unrealistically increases the difficulty of cutting, but if the whole cutting action is to be completed, the cutting action must be completed under actual conditions (PVC sampling tube containing hydrate).

### 5 Experiments

#### 5.1 Test process

As shown in Fig. 14, the working process of the core sample pressure maintaining transfer device is as follows:

(A) Connect the gravity sampler and the deep-sea sample high-fidelity processing system via a hoop, turn on the temperature and pressure holding device, and adjust the temperature and pressure of the deep-sea sample processing system to the same point as the sampling point.

(B) Open the ball valve to connect the gravity sampler with the deep-sea sample high-fidelity processing system, start the long-stroke push device, push the grab rod to the sample tube joint, and rotate the grab rod to make the connection between them secure.

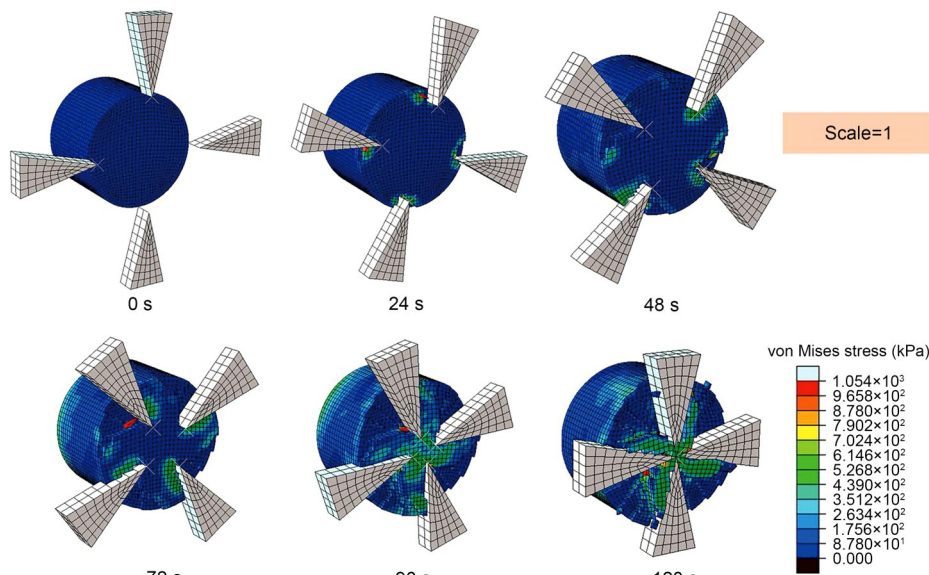
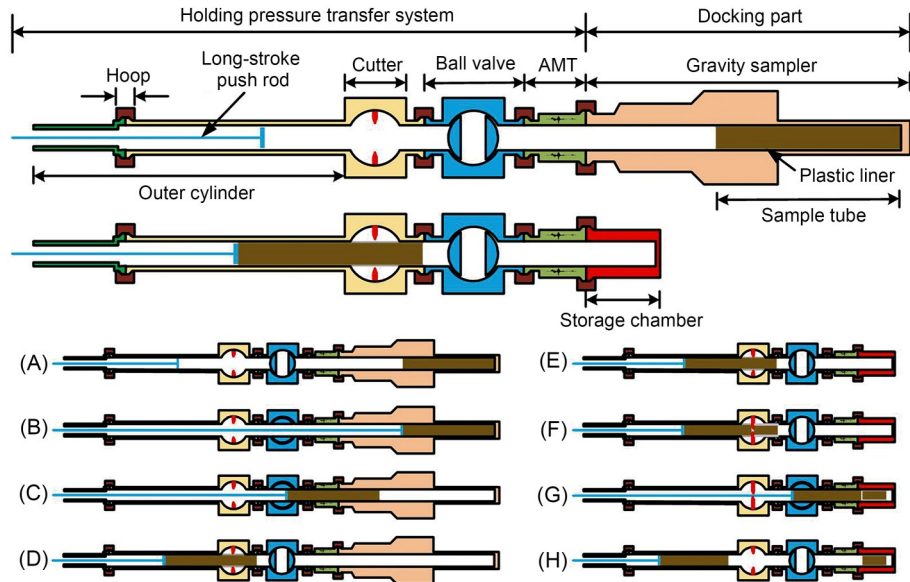


Fig. 13 Single cutting simulation



**Fig. 14** Hydrate sample processing of the hydrate samples pressure-holding transfer system (AMT: acoustic measurement tank)

(C) Maintain the same temperature and pressure, retract the gripper to the CT, reduce the speed, and rotate the gripper while opening the CT for scanning to obtain the internal structure of the sample.

(D) Wait until the CT scan is complete, continue to retract the gripper with the sample tube to the high-fidelity sample cutting device, and stop retracting. Then close the ball valve.

(E) Open the hoop and disconnect the gravity sampler from the deep-sea sample high-fidelity processing system. Then the sample storage compartment is connected to the deep-sea sample high-fidelity processing system.

(F) Hold the long-stroke pushing device still, open the clamping mechanism of the deep-sea sample high-fidelity cutting device to fix the sample tube, and open the cutting mechanism to cut the sample tube.

(G) Wait for the sample tube to be cut. Open the ball valve and push forward the sample section to be cut as required into the sample storage compartment.

(H) Retract the gripper and close the ball valve. The sample section to be cut is already in the storage compartment. Close the valve in the sample storage compartment and disconnect the clamp. The cutting is completed in one step. Repeat the above steps to cut the sample section again.

To complete the cutting, it is necessary to initialize the cutting device to determine the position of the cutting knife. During the design process, the range of

motion of the cutter is determined by the interval of the parameter equation of the Archimedes spiral on the spiral grooved plate, and the upper and lower limits of the interval can be used to limit the cutter. Without a reducer, control the No. 1 motor to rotate to overload, and the knife is centered. To avoid the cutters colliding with each other in error, a 3-mm circumferential safety clearance is set. After the operation of reserved safety clearance is completed, the cutting can be recycled. Table 4 shows the setup parameters for each step. The revolving cutting process includes rotating cutting and returning to the maximum diameter, as shown in Fig. 15.

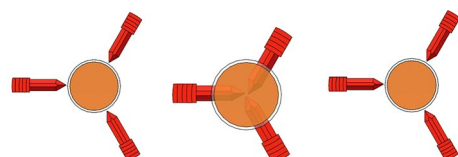


**Fig. 15** Complete single cut process schematic

It should be noted that  $W_1$  is the speed of cutting of the cutter limit plate, and  $W_2$  is the speed of cutting of the spiral groove plate. When the values of  $W_1$  and  $W_2$  are negative, they all represent the anti-clockwise rotation of the motor.  $W_1+W_2$  represents the superposition speed, which determines the feed and returns the speed of the cutter. The value of  $W_1+W_2$  represents rotary feed when it is negative and rotary withdrawal when it is positive.

## 5.2 On-site cutting effect

We cut at the in-situ pressure and see that the pressure gauge (top left corner in Fig. 16) shows up to 30 MPa, and this pressure is maintained for at least 12 h (Gao et al., 2020). During the test, the team connected ball valves at both ends of the cutting device, pushed the pressure from the top with a pneumatic booster pump, and maintained the pressure with ball valves. The state of the cutting knives inside the high-fidelity cutting device is shown in Fig. 16, uniformly distributed, and due to the compensating design of the length of the cutting knives, the circles formed by the tip of the three cutting knives coincide with the centers of the sample tube. The sample tube cut by the high-fidelity cutting device is shown in the lower right corner of Fig. 16. The cut-out of the sample tube is smooth, and the minimum width of the sample pipe section can be much less than 2 cm, so that almost any length of the sample tube can be cut.

When the inside of the sample tube is filled with sediment, the whole cutting surface and sediment of the sample tube are also very smooth. The cutting surface characteristics can be summarized as follows: smooth cutting surface, smooth incision, little sediment disturbance, and almost no chip residue. Therefore, in general, the cutting effect achieved by the cutting path of the cutter is very satisfactory.

## 6 Discussion

Hydrate samples separated by conventional means generally no longer have the same characteristic properties once they are onshore as they did on the sea floor. Hydrates decompose at elevated temperatures and reduced pressures, so conventional hydrate samples lose their characteristics once they are onshore. Even if some pressure-holding samplers maintain the pressure, the change in temperature and the lack of associated sample transfer and cutting processing devices

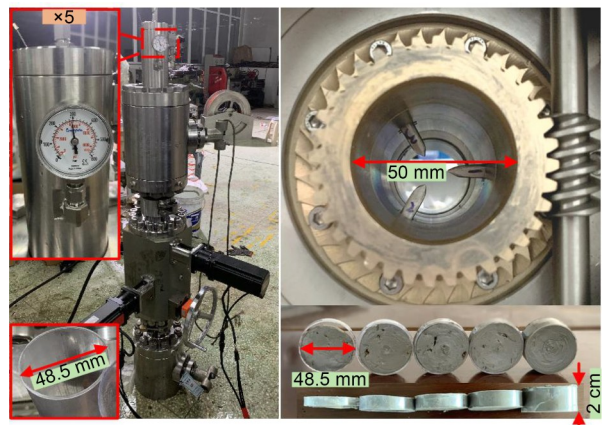


**Fig. 16** On-site installation and cutting effect demonstration

make it impossible to perform laboratory tests in the same state as on the sea floor.

In this study, a high-fidelity cutting device for in-situ cutting of hydrate sampling tube was designed, mainly based on the principle that the Archimedes spiral is an isometric spiral. The electronic control system controls servo motors to drive the worm gears and worms so that the cutter can move in the spiral groove according to the Archimedes spiral line. This cutter motion path results in less cutting disturbance for the hydrate samples and makes precise control possible due to the determination of the motion path. The sample tube had an outside diameter of 48.5 mm and a total of 10 cuts were made. The cut sections are shown in Fig. 17. Most of the cut sections are very flat, with only two or three of them producing a larger disturbance. In general, the disturbance level of the cut sections is well controlled.

The single cutting time is only 2 min, which achieves high cutting efficiency while maintaining the quality of the cut. In order to save time, the differential speed of tool retraction can be increased to achieve the fastest retraction to the original position within 20 s, so that the single cycle cutting time is 140 s. The whole process is controlled by the upper computer to achieve a rapid cycle of cutting. During the sea trial,

**Table 4** Motor setup table for cutting process

Step	Action	Time (s)	W1 (r/min)	W2 (r/min)	W1+W2 (r/min)
1	Cutting knife centering	—	-180	0	-180
2	Reserving a safe distance	9	540	0	540
3	Backing to maximum diameter	30	2700	0	2700
4	Cutting	120	-2295	1620	-675
5	Repeating steps 3 and 4				



Fig. 17 Cutting sections of in-situ sample tubes

the pressure fluctuation of both core holding pressure transfers was 1.04%. In addition to the role of the pressure maintenance system, the good sealing performance of all parts, including the high-fidelity cutting device, jointly achieved this goal, so that the result achieved far exceeded the design goal (a pressure fluctuation of less than 10%).

Thanks to the use of the electronic control system, the control of the servo motors became simple and reliable, and the corresponding cutting function could be better realized. Defining and encapsulating the buttons on the upper computer interface enables one-button cutting and fallback. The upper computer interface can dynamically display the position of the core tube in real time, making it possible to cut any length of sample tube within a section. To avoid cutting into the entire rock, an emergency cutback function was designed to avoid the loss of in-situ environmental pressure due to reloading. The main difficulty in recalibrating the tool without equipment disassembly is the presence of ambient pressure and unseen material in the equipment. Thanks to the Archimedes spiral, which can be calculated precisely, improvements at the software control level can be made to obtain the desired results.

In April 2021, we conducted a sea trial test in the South China Sea and performed two pressure-holding transfer tests (including many steps such as transfer, cutting, scanning, and sample transfer storage). The first core was processed from 7:04 a.m. to 9:26 a.m. for about 2.5 h, during which the pressure varied from 22.07 to 21.84 MPa, and the pressure fluctuation rate was calculated to be 1.04%. The second core was processed from 10:04 a.m. to 4:36 p.m. for about

6.5 h, during which the pressure varied from 20.18 to 19.97 MPa, and the calculated pressure fluctuation rate was 1.04%. In the PCATS, developed by Geotek Ltd., UK in the HYACINTH program, only 15% pressure range is guaranteed. During China's Twelfth Five-Year Plan period, the pressure fluctuation index of pressure-holding transfer equipment is 20%. Compared with previous products, this equipment has made great progress in respect of pressure fluctuation, and pressure fluctuation is far less than 10% specified in its design. The high-fidelity cutting device designed has reached the current international advanced level in controlling pressure fluctuation. Similar advanced performance is reflected in the control of temperature fluctuations, which do not exceed 0.5 °C during sea trials. Because of the function of the automatic temperature control system, the hydrate will not decompose during the cutting process. Under the condition that the temperature and pressure are strongly controlled, the high-fidelity cutting of the hydrate has achieved initial success.

To better build a high-fidelity cutting device system, the corresponding drive motor selection is the key point, so the clamping force is calculated to provide sufficient driving force to make the in-situ cutting go smoothly. Through force analysis, the relationship between the forces required for the cutting tool and the driving torque is obtained. Combined with cutting analysis, the force required for cutting can be calculated and the driving torque can be calculated by establishing the equation. Then the servo motors can be selected according to the transmission characteristics of worm gear and worm. The simulation analysis reduces the difficulty of simulation by assuming all sample tubes as PVC tubes, because the strength of PVC tubes is greater than that of hydrate. The simulation results show that the cutting of a PVC pipe can be realized, and the cutting under real circumstances is possible.

## 7 Conclusions

This research investigated the mechanical structure design and electrical control system construction of the high-fidelity cutting device. When cutting by mechanical means, the generation of chips is inevitable. The anti-blocking design was included, preventing cutting chips from entering the spirally grooved disk and

causing cutting blockage. Pre-written procedures rather than manual proofreading realized the initialization and step cycle of the cutting process, which improves the convenience dramatically. Besides, accuracy is improved by orders of magnitude compared with a mechanical counter.

The equipment designed in this study can be used for high-fidelity cutting of deep-sea samples, thus providing important technical guarantees for the study of hydrates. It significantly supports research on marine energy and marine sediment cores. The hydrate is disturbed as little as possible, and is maintained as far as possible at its in-situ state.

### Acknowledgments

This work is supported by the Key R&D Program of Zhejiang Province (No. 2021C03183), the Key Special Project for Introduced Talents Team of Southern Marine Science and Engineering Guangdong Laboratory (Guangzhou) (No. GML2019ZD0506), and the National Natural Science Foundation of China (No. 2017YFC0307500).

### Author contributions

Hai ZHU designed the device mainly. Hai ZHU and Jia-wang CHEN processed the data. Hai ZHU and Zi-qiang REN drafted the manuscript. Pei-hao ZHANG, Qiao-ling GAO, and Chun-ying XU helped organize the manuscript. Xiao-ling LE helped with the simulation analysis of cutting. Kai HE, Peng ZHOU, Feng GAO, and Yu-ping FANG helped design the device. Hai ZHU revised and finalized the paper.

### Conflict of interest

Hai ZHU, Jia-wang CHEN, Zi-qiang REN, Pei-hao ZHANG, Qiao-ling GAO, Xiao-ling LE, Chun-ying XU, Kai HE, Peng ZHOU, Feng GAO, and Yu-ping FANG declare that they have no conflict of interest.

### References

- Attanasio A, Ceretti E, Fiorentino A, et al., 2010. Investigation and FEM-based simulation of tool wear in turning operations with uncoated carbide tools. *Wear*, 269(5-6): 344-350.  
<https://doi.org/10.1016/j.wear.2010.04.013>
- Dai S, Santamarina JC, 2014. Sampling disturbance in hydrate-bearing sediment pressure cores: NGHP-01 expedition, Krishna-Godavari Basin example. *Marine and Petroleum Geology*, 58:178-186.  
<https://doi.org/10.1016/j.marpetgeo.2014.07.013>
- Gao QL, Chen JW, Liu JB, et al., 2020. Research on pressure-stabilizing system for transfer device for natural gas hydrate cores. *Energy Science & Engineering*, 8(4):973-985.  
<https://doi.org/10.1002/ese3.562>
- Hayashi T, Sakurai S, Shibanuma K, et al., 2014. Development of remote pipe cutting tool for divertor cassettes in JT-60SA. *Fusion Engineering and Design*, 89(9-10):2299-2303.  
<https://doi.org/10.1016/J.Fusengdes.2014.04.026>
- Hoang AQ, Aono D, Watanabe I, et al., 2021. Contamination levels and temporal trends of legacy and current-use brominated flame retardants in a dated sediment core from Beppu bay, southwestern Japan. *Chemosphere*, 266: 129180.  
<https://doi.org/10.1016/j.chemosphere.2020.129180>
- Hyodo M, Li YH, Yoneda J, et al., 2014. Effects of dissociation on the shear strength and deformation behavior of methane hydrate-bearing sediments. *Marine and Petroleum Geology*, 51:52-62.  
<https://doi.org/10.1016/j.marpetgeo.2013.11.015>
- Kamruzzaman M, Dhar NR, 2009. Effect of high-pressure coolant on temperature, chip, force, tool wear, tool life and surface roughness in turning AISI 1060 steel. *Gazi University Journal of Science*, 22(4):359-370.
- Li JF, Ye JL, Qin XW, et al., 2018. The first offshore natural gas hydrate production test in South China Sea. *China Geology*, 1(1):5-16.  
<https://doi.org/10.31035/cg2018003>
- Li L, Kishawy HA, 2006. A model for cutting forces generated during machining with self-propelled rotary tools. *International Journal of Machine Tools and Manufacture*, 46(12-13):1388-1394.  
<https://doi.org/10.1016/j.ijmachtools.2005.10.003>
- Lukin N, Moura RT, Alves M, et al., 2020. Analysis of API S-135 steel drill pipe cutting process by blowout preventer. *Journal of Petroleum Science and Engineering*, 195:107819.  
<https://doi.org/10.1016/j.petrol.2020.107819>
- Moore MT, Phillips SC, Cook AE, et al., 2020. Improved sampling technique to collect natural gas from hydrate-bearing pressure cores. *Applied Geochemistry*, 122:104773.  
<https://doi.org/10.1016/j.apgeochem.2020.104773>
- Pang BX, Wang SY, Jiang XX, et al., 2019. Effect of orbital motion of drill pipe on the transport of non-Newtonian fluid-cuttings mixture in horizontal drilling annulus. *Journal of Petroleum Science and Engineering*, 174: 201-215.  
<https://doi.org/10.1016/J.Petrol.2018.11.009>
- Parkes RJ, Sellek G, Webster G, et al., 2009. Culturable prokaryotic diversity of deep, gas hydrate sediments: first use of a continuous high-pressure, anaerobic, enrichment and isolation system for subseafloor sediments (Deepisobug). *Environmental Microbiology*, 11(12):3140-3153.  
<https://doi.org/10.1111/j.1462-2920.2009.02018.x>
- Priest JA, Druce M, Roberts J, et al., 2015. PCATS triaxial: a new geotechnical apparatus for characterizing pressure cores from the Nankai Trough, Japan. *Marine and Petroleum Geology*, 66:460-470.  
<https://doi.org/10.1016/j.marpetgeo.2014.12.005>
- Ren ZQ, Chen JW, Gao QL, et al., 2020. The research on a driving device for natural gas hydrate pressure core. *Energies*, 13(1):221.  
<https://doi.org/10.3390/en13010221>
- Saelzer J, Berger S, Iovkov I, et al., 2020. In-situ measurement

- of rake face temperatures in orthogonal cutting. *CIRP Annals*, 69(1):61-64.  
<https://doi.org/10.1016/j.cirp.2020.04.021>
- Toussaint R, 2008. Pipe Cutting Apparatus. US Patent 7406769.
- Tsuchiya M, Nomaki H, Kitahashi T, et al., 2019. Sediment sampling with a core sampler equipped with aluminum tubes and an onboard processing protocol to avoid plastic contamination. *MethodsX*, 6:2662-2668.  
<https://doi.org/10.1016/J.MEX.2019.10.027>
- Wang Y, Xu TF, Zhang PY, et al., 2020. Experimental investigation of coolant selection and energy efficiency analysis during gas hydrate-bearing sediment freeze-sampling. *International Journal of Refrigeration*, 120: 221-236.  
<https://doi.org/10.1016/j.ijrefrig.2020.07.027>
- Ye JL, Qin XW, Qiu HJ, et al., 2018. Preliminary results of environmental monitoring of the natural gas hydrate production test in the South China Sea. *China Geology*, 1(2):202-209.  
<https://doi.org/10.31035/cg2018029>
- Ye JL, Qin XW, Xie WW, et al., 2020. The second natural gas hydrate production test in the South China Sea. *China Geology*, 3(2):197-209.  
<https://doi.org/10.31035/cg2020043>
- Yen YC, Söhner J, Lilly B, et al., 2004. Estimation of tool wear in orthogonal cutting using the finite element analysis. *Journal of Materials Processing Technology*, 146(1): 82-91.  
[https://doi.org/10.1016/S0924-0136\(03\)00847-1](https://doi.org/10.1016/S0924-0136(03)00847-1)
- Yi J, Qian YP, Shang ZQ, et al., 2017. Design of cutting head for efficient cutting machine of thin-walled stainless steel pipe. *Procedia Engineering*, 174:1276-1282.  
<https://doi.org/10.1016/j.proeng.2017.01.302>
- Yoneda J, Oshima M, Kida M, et al., 2019. Permeability variation and anisotropy of gas hydrate-bearing pressure-core sediments recovered from the Krishna-Godavari basin, offshore India. *Marine and Petroleum Geology*, 108: 524-536.  
<https://doi.org/10.1016/j.marpetgeo.2018.07.006>
- Zhang PH, Chen JW, Gao QL, et al., 2019. Research on a temperature control device for seawater hydraulic systems based on a natural gas hydrate core sample pressure-retaining and transfer device. *Energies*, 12(20):3990.  
<https://doi.org/10.3390/en12203990>
- Zhao JF, Song YC, Lim XL, et al., 2017. Opportunities and challenges of gas hydrate policies with consideration of environmental impacts. *Renewable and Sustainable Energy Reviews*, 70:875-885.  
<https://doi.org/10.1016/j.rser.2016.11.269>
- Zhu H, Chen JW, Lin Y, et al., 2018. A high pressure holding and cutting device for sampling tube of natural gas hydrate. OCEANS 2018 MTS/IEEE Charleston, p.1-4.  
<https://doi.org/10.1109/OCEANS.2018.8604734>
- Zhu ZL, Buck D, Guo XL, et al., 2020. Cutting performance in the helical milling of stone-plastic composite with diamond tools. *CIRP Journal of Manufacturing Science and Technology*, 31:119-129.  
<https://doi.org/10.1016/j.cirpj.2020.10.005>

# *Electronically Controlled Deep Sea Sampling Tube Pressure Maintaining Cutting Device Capable of Long-term Use*

Hai Zhu, Jiawang Chen, Yuan Lin, Peihao Zhang, Ziqiang Ren, Xiaoling Le, Jing Xiao, Ziang Feng

Ocean College, Zhejiang University, Zhoushan, 316021, China

\*Corresponding author: simaizhu@icloud.com

## I. INTRODUCTION

A kind of sample tube pressure-keeping cutting device is designed, which is feasible from the perspective of manufacturing and assembly, and the relevant Ansys simulation is carried out to verify the rationality of the structure. The biggest breakthrough is that one installation can realize multiple cutting of sampling pipes, eliminating the step of cleaning sea mud in the pipes. In addition, the redesign of the cutting knife and the re-selection of the outer cylinder material reduced the overall size to 71.9% and the mass to 22.3%. Anti-sludge blocking design was carried out, thus realizing long-term use design.

## II. DEVICE DESIGN

### A. Design indicators

As an important part of the pressure maintaining transfer device, the cutting device requires a smooth, undisturbed rapid cutting of the sampling tube at an in-situ pressure of 30 MPa. The design purpose and design indicators of this equipment were proposed<sup>[1-2]</sup>:

- Working pressure: 30Mpa;
- Operating temperature: 2-4 °C;
- Pressure change during transfer:  $\leq 20\%$ ;
- Cause no secondary pollution to the sample;
- Controllable cutting process;
- Shorten the cutting time as soon as possible.



Fig. 1 Overall drawing of pressure maintaining transfer device

### B. Institutional composition

The cutting device requires a smooth, undisturbed rapid cutting of the sampling tube at an in-situ pressure of 30 MPa. The sampling tube high pressure cutting device mainly comprises a clamping mechanism and a cutting mechanism. The subsea sampling tube is transported to the operating vessel for pressure-holding cutting to obtain small samples for laboratory research.

The clamping mechanism is intended to assist other mechanisms on the pressure maintaining transfer device to further secure the sampling tube for smoother cutting. It is shown in the left half of Figure 2.

The cutting mechanism aims to achieve a smooth and controllable cutting effect without the sampling tube rotating. The mechanism adopts a knife-rotating method to meet the requirements. It is shown in the right half of Figure 2.

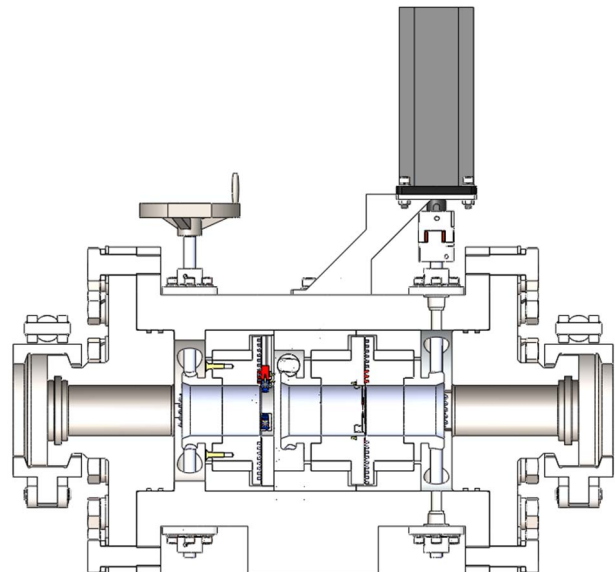


Fig. 2 The whole half section of the high pressure cutting device.

The cutting device not only requires good cutting results, but also needs to be simple and feasible in both assembly and manufacturing. The previous sampling tube high pressure cutting device was optimized, and many previous unreasonable designs including the clamping mechanism, the cutting mechanism and the cylinder were solved.

### C. Working principle

The sampling tube high pressure cutting device mainly comprises a clamping jaw, a spiral groove disk and a fixed disk, wherein the fixed disk is kept motionless, and the spiral groove disk is operated by a manual spoke, and the sample tube can be

finally clamped by controlling the number of rotation turns after feeding 5mm per rotation turn.

The basic principle of the cutting mechanism is similar to that of the clamping mechanism, except that a fixed disk is replaced by a freely rotatable disk. This makes the cutter have a certain cutting speed while feeding. The rotating speed is determined by the cutting disc (i.e. the free rotating disc), and the advancing and retreating speed and advancing and retreating speed of the cutter are determined by the differential speed between the spiral groove disc and the spiral groove disc.



Fig. 3 Test piece for cutting mechanism

### III. ELECTRONIC CONTROL AND CURVE DESIGN

The movement of the cutter is controlled by two servo motors, model number DELTA ECMA-J10807SS, equipped with DELTA ASD-A2-0743-M. The control mode of servo motor selects the speed control mode, and the laboratory engineer is responsible for designing the upper computer for interface control. Combined with the characteristics of the Archimedes spiral, it can precisely control the advance and retraction speed of the cutter and the rotational speed of the circumferential cutting.

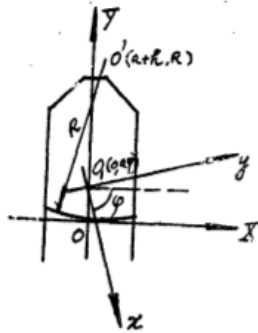


Fig. 4 Round involute meshing

As a flat thread type three-jaw chuck disk curve, the following conditions must be met: when the wire is rotated at any angle, the displacement of the three jaws in the groove of the disk body should be equal (the three-claw movement is equal). Thus, after the disk is rotated for one revolution, the claw arc is moved to the adjacent one of the coils, and the displacement of the jaws in the slot is just the pitch of the coil. Therefore, if the arc is an equidistantly distributed jaw, not only can the disc be embedded in any position, but also the teeth arc between the discs and the coils can be meshed at the same time, so the coil The pitch of the flat two threads must remain constant.

In order to solve such problems, the wire curve is intended to adopt an involute curve. Considering that the claw arc is easy to process under the existing equipment conditions, the arc curve is selected as a semi-circular arc of the equidistant distribution, and the distance between the core and the claw width is  $a+h$ , and the arc is half.  $R$ , the distance between the two adjacent arcs is  $2\pi a$ .

On the wire, take the core of the wire as the coordinate origin, and establish the coordinate system  $XOY$  (Fig. 4), so that the initial position of the core  $O'$  in the claw arc is  $(a+h, R)$ , and the core of the claw width is in  $OY$ . On the shaft. The wire curve is the moving coordinate system  $XO_1Y$  after the coordinate system  $XOY$  passes the positive translation distance  $a\phi$  to the  $OY$  axis and then rotates the angle  $\phi$  clockwise around the new coordinate origin  $O_1$ . Let  $h = 0$ , then the curve equation of the wire curve:

$$x = a \cos \phi + a \phi \sin \phi$$

$$y = a \sin \phi - a \phi \cos \phi$$

### IV. OPTIMIZATION OF DESIGN

#### A. Cutting knife redesign

The length of the cutting knife is related to the depth of precession, that is, to the diameter of the sampling tube. In addition, it is necessary to ensure the engagement of the three teeth, so the length of the cutting knife is related to the diameter of the sampling tube and the number of teeth engaged. The length of the cutting knife has been reduced from 79mm to 43 mm. The cutter head of the cutting knife has also been redesigned. The cutter head needs to be able to be retracted repeatedly so as not to affect the movement of the sampling tube inside the cutting device and at the same time to reach the center of the circle of the sampling tube.

Because the wall of the sampling tube is very thin, it becomes more reasonable and reliable to design the cutter head as a blade-like sheet. As shown in the Figure 6, it can be seen that the cutting section is flat.



Fig.5 Version comparison of cutting Knife



Fig.6 Experimental cutting

### B. Optimization of overall size and weight

The redesign of the cutter and the re-selection of the outer cylinder material reduced the overall size to 71.9% and the mass to 22.3%. Thanks to the material selection of the outer cylinder changed from the original 17-4PH to 7075 aluminum alloy, the overall quality has been greatly reduced. A test device was made to test the principle and feasibility in practice. As shown in the figure 6, the device successfully cut the thick sampling tube with smooth and flat cutting surface. By controlling the two servo motors, the circumferential rotation speed and the radial feed speed can be controlled.



Fig.7 Cutting experimental device and cutting section

### V. LONG-TERM USE DESIGN

Since the sampling tube is mainly composed of seabed silt, it will enter the groove of the spiral groove disc through the gap during cutting, affecting the precession of the cutting knife. Therefore, a cutter plug is designed to prevent silt from entering. Due to this design, it is not necessary to disassemble the sludge for cleaning after each cutting is completed. Therefore, the long-term use design is realized. Because the new type of cutting knife produces little chips, which is important for cutting in enclosed space. Because if the amount of chips is too large, it needs to be removed frequently to remove the chips, which affects the multiple uses of the cutting device.

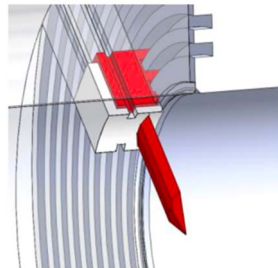


Fig.8 Anti-sludge blocking design

### VI. CUTTING EFFECT EVALUATION

For the description of the quality of the cutting surface, some indicators are often involved, such as surface roughness, cutting disturbance zone scale, slit width, slit perpendicularity, slit surface finish, brittle fracture rate, slag loading rate, heat affected zone width. Different cutting parameter settings correspond to different cutting surface features. The description of the cutting surface and how to link the cutting parameters with the cutting surface features are the focus of research. A set of cutting specification manuals is proposed to give

corresponding ideal cutting parameter settings for different samples.

Seabed sampling objects are generally seabed sediments and drilling cores. The rheological properties of the samples affect the quality of the cut surface of the sample. Good cutting surfaces are more advantageous for subsequent laboratory studies. It is important to study how to ensure the quality of the cut surface for different samples. There is a strong relationship between the mechanical properties of seabed sediments and their concentrations, so it is necessary to explore the effect of concentration on the rheological properties of bentonite suspensions.

The clay suspension system is more complex, and the clay mineral particles are charged sheet-like nanoscale particles. The surface of the particle has a permanent negative charge. The charge on the edge changes significantly with pH: positive in acidic environments and negative in alkaline conditions. Therefore, in the clay suspension, the clay particles are subjected to a complex electric double layer electrostatic force, and the interaction force mainly has an electrostatic attraction between the face and the edge and an electrostatic repulsion between the faces. In order to achieve the balance between electrostatic force and van der Waals force (collectively referred to as DLVO force), a structure such as face-to-face and face-edge can be formed between the particles to make the clay suspension into a gel state<sup>[3-4]</sup>.

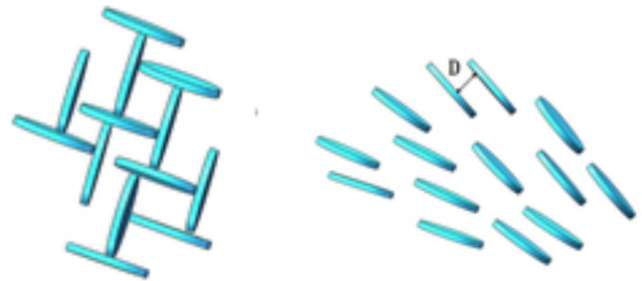


Fig.9 Microstructure diagram of bentonite clay particles

Seabed sediments of different depths have different compositions. Typically, the main components of the seabed core are clay and terrigenous debris. In terms of the depth and location of the gas hydrate, its storage environment is shale deposits and the main component is a clay suspension.

In the past, the cutting of the core does not consider the mechanical properties of the sample, which may cause some unsatisfactory cutting effects, such as disturbance, brittle fracture, and slag. How to reduce such undesired conditions requires exploration of the mechanical properties of the sample.

The combination of engineering practical problems and theoretical research complements each other. The core cutting device can be used for cutting most cores. The introduction of rheology provides a reference for the scientific setting of cutting parameters.

## VII. REAL EFFECT

This high pressure pressure cutting device has not been made into real material, which is used for the actual gas hydrate sampling pipe cutting. We believe that with this design, better cutting effects will be presented. The new device will be produced by the end of 2019 and put into use. The current state is that the processing drawings have been produced, and the actual cutting effect cannot be provided in this paper at the current stage of processing.



Fig.10 The previous version of the cutting device

The follow-up work will continue, and the use effect of relevant devices will be further reflected in the subsequent work. The cutting device will be processed in the following period of time, and there is reason to believe that better cutting effect will be shown.

## VIII. CONCLUSION

Compared with the existing technology, the main benefits of this work are:

1. New material selection and cutting knife design have greatly reduced the weight and size of the cutting device.

2. The newly adopted cutter plug makes it difficult for cuttings and sludge to enter the spiral groove disc, which makes multiple cuts possible.

3. The use of servo motor allows the cutting process to be controlled by the upper computer, which is accurate and convenient.

4. The new cutting knife can be used for cutting thin pipe walls, expanding the application range of the device.

## ACKNOWLEDGMENT

Thanks to Professor Chen Jiawang and Professor Lin Yuan for their guidance, thanks to the help of the lab team and the engineers, this is an unforgettable time.

## REFERENCES

- [1] Jiawang Chen et al, pressure maintaining system of pressure maintaining transfer device for natural gas hydrate. journal of marine technology, 2017 ( 02 ): 23 - 27.
- [2] Jiawang Chen et al, study on pressure characteristics of gas hydrate pressure maintaining subsampler. ocean engineering, 2017 ( 05 ): pp. 103 - 109.
- [3] Lin Y , Phan-Thien N , Lee J B P , et al. Concentration Dependence of Yield Stress and Dynamic Moduli of Kaolinite Suspensions[J]. Langmuir, 2015, 31(16):4791-4797.
- [4] Laxton, P. B.; Berg, J. C. Relating clay yield stress to colloidal parameters. J. Colloid Interface Sci. 2006, 296, 749–755.

# A high pressure holding and cutting device for sampling tube of natural gas hydrate

Hai Zhu, Jiawang Chen, Yuan Lin, Peihao Zhang, Huangchao Zhu, Ziqiang ren

Ocean College, Zhejiang University, Zhoushan, 316021, China

\*Corresponding author: simaizhu @icloud.com

A high pressure maintaining cutting device for natural gas hydrate sampling tubes is designed, which is mainly used for pressure maintaining cutting of deep sea sampling tubes. The main mechanism is designed in detail, some advantages of this design are expounded, and the operation sequence of the cutting mechanism is introduced. Since the design and processing have not been completely completed, ANSYS simulation of some related parts has been carried out. The advantages of current design over previous generation products are summarized, and the existing problems are also explained.

**Keywords**—cutting; simulation; design

## I. INTRODUCTION

The natural gas hydrate sampler is a powerful tool for studying the characteristics of hydrate in different regions. The gas hydrate sample pipe is transported to the operation ship for pressure maintaining cutting to obtain small samples for laboratory research. The cutting device requires minimal possible cutting disturbance while being able to maintain the same pressure and temperature as the sampling point. A new high pressure cutting device for gas hydrate sampling tube is designed, which includes clamping mechanism, cutting mechanism, high pressure inner cylinder, high pressure cylinder, end cover, temperature control system, pressure maintenance system and motor control board.

## II. DESIGN

### A. Main body design

The cutting device requires a smooth, undisturbed rapid cutting of the sample tube at an in-situ pressure of 25 MPa, which puts forward the following requirements for the cutting device:

1. The cutting device must be resistant to high internal pressure;
2. Simple structure, avoid redundancy;
3. Each part of that cut device connected with the transfer device require higher sealing performance;
4. The sample cutting device does not cause secondary pollution to the sample;
5. Minimize the disturbance of the sample during the cutting process;
6. The cutting process is controllable and the cutting depth is accurately controlled;
7. Shorten the cutting time as soon as possible.

The following is the design chart of high pressure preservation cutting device for gas hydrate sampling tube.

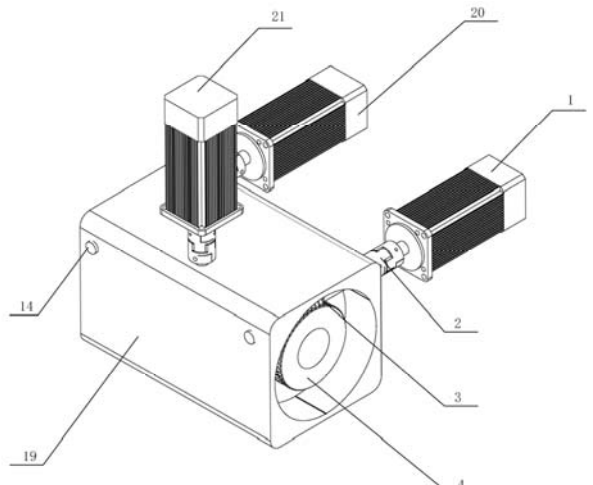


Fig. 1. The overall appearance of the high pressure cutting device

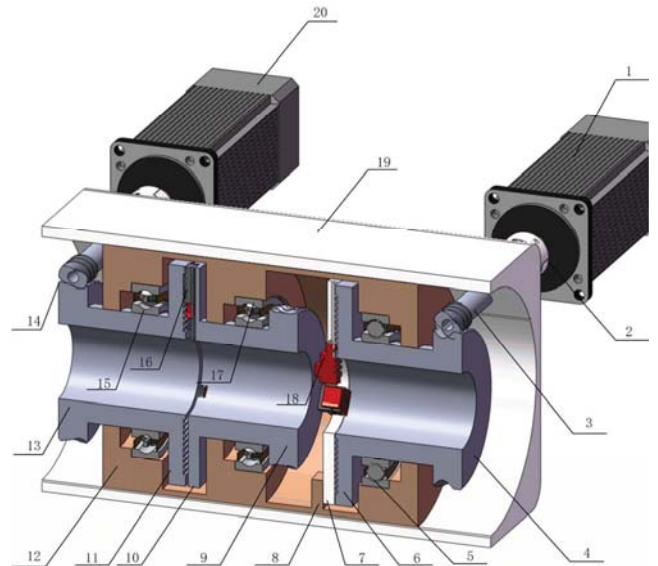


Fig. 2. The whole half section of the high pressure cutting device.

1. Clamping motor, 2. Coupling, 3. Clamping worm, 4. Clamping worm wheel, 5. Clamping mechanism bearing, 6. Clamping spiral groove plate, 7. Fixed disk, 8. High pressure cylinder, 9. Cutting worm wheel, 10. Cutting disc, 11. Cutting spiral groove plate, 12. High pressure inner cylinder, 13. Feed worm wheel, 14. Feed and back worm, 15、17. Cutting mechanism bearing, 16. Cutting head, 18. Claw, 19. High

pressure outer cylinder, 20. Feed motor, 21. Circumferential cutting motor.

The working process of the high pressure cutting device for deep sea sediment pressure sampling and transferring is as follows:

- 1) When the sample tube reaches the specified position, start the clamping motor, fast radial movement, until it is about to clamp through the control panel switch to slow clamping.
- 2) Wait until the clamp clamping, turn off the clamping motor, complete clamping.
- 3) Start the feed motor so that the cutter head is fed quickly. After reaching the surface of the sample tube, the motor switches to low speed.
- 4) Slow feed, fast circumferential cutting at the same time, wait for cutting is completed, stop feeding.
- 5) Adjust that rotating speed of the feed motor, and returning the cutter head.
- 6) Rotate the clamping motor in the opposite direction so that the clamp releases the sample tube
- 7) Cutting is completed, pushed to the designated position again, repeated cutting operation.

#### B. Design of main movement mechanism

A new high-pressure cutting device for natural gas hydrate sampling tube is designed, which mainly includes clamping mechanism and cutting mechanism.

- The clamping mechanism comprises a claw, a clamping spiral groove plate, a fixed disk, a clamping bearing and a clamping motor. The clamping spiral groove plate and the clamping worm wheel are integrally connected, and the clamping bearing supports the high pressure inner cylinder, and the bearing is a deep groove ball bearing and oil lubrication. The guide groove is mounted on the fixing plate so that the jaws are directly loaded into the fixing plate. Three plate-like bodies are formed inside the high-pressure inner cylinder, and holes are formed therein for fixed connection with the fixing plate by bolts. Archimedes spiral fit between the jaws and the spiral grooved disk. The relative rotation of the jaws is determined by the Archimedes spiral.

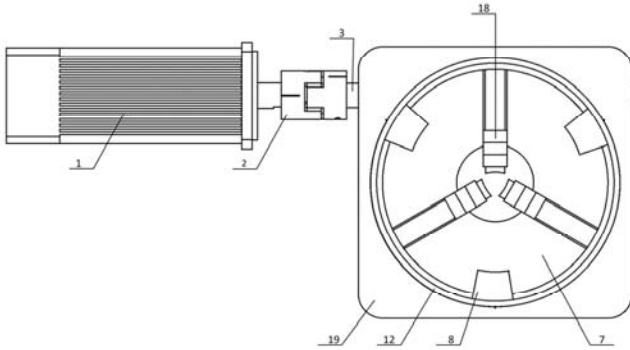


Fig. 3. Schematic diagram of clamping mechanism

- The cutting mechanism comprises a cutting disc, a cutting spiral groove plate, a cutter head, a cutting bearing, a circumferential rotating motor, and a front and rear knife motor; the guiding groove is located on

the cutting disc, the spiral groove on the cutter head cooperates with the spiral groove plate, and the bearing supports the high pressure inner cylinder. The spiral groove plate and the cutting disk cut the forward and reverse worm wheels by a circumferentially rotating worm wheel, and the cutting spiral groove is made of an Archimedes screw; the worm gear mechanism is included in the cutting mechanism. In the clamping mechanism, the worm is connected to the high pressure outer cylinder by a contact dynamic seal, and the worm gear mechanism is driven by an external motor. The high-pressure outer cylinder and the end cover are bolted, and the internal structure of the high-pressure cylinder is consistent with the spiral groove plate. In the design, the high pressure cylinder is sufficient to withstand a design pressure of 25 MPa; the motor control panel controls the rotational speeds of the forward and reverse motors and the circumferential rotating motor to determine the peripheral speed and radial feed rate of the cutting mechanism, and an electric motor can also be used. The control panel controls the clamping speed of the clamping mechanism.

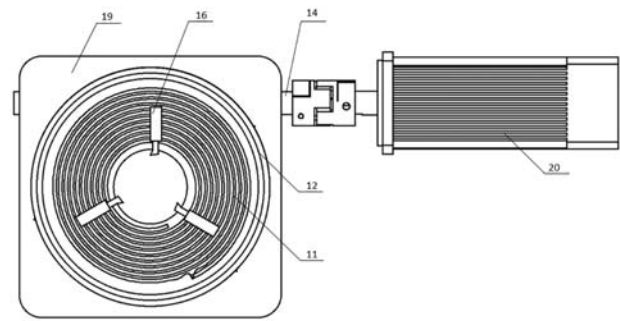


Fig. 4. Schematic diagram of left half of cutting mechanism

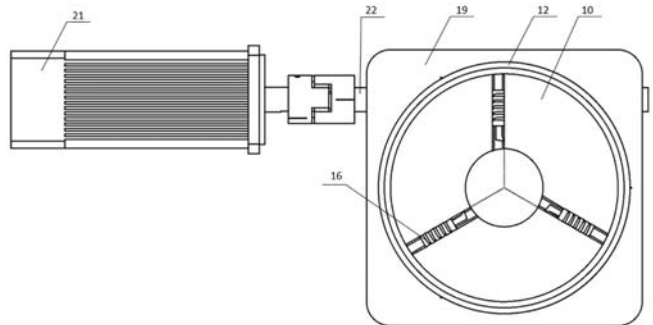


Fig. 5. Schematic diagram of right half of cutting mechanism

#### III. ANSYS SIMULATION

Since the design took a long time, it is currently in the testing and processing stage and has not yet been formally worked. In order to make up for the shortage of physical objects, the design team carried out ANSYS simulation analysis. It mainly includes the simulation of cutter head and

turbine. the simulation results show that the material selection and design are reasonable.

#### A. Modeling

Solidworks is used to establish a three-dimensional model and is imported into ANSYS for simulation analysis. The material properties of the cutter bar include elastic modulus  $E = 210$  GPa, poisson's ratio  $\nu = 0.3$ , yield strength  $y = 1350$  MPa, and density  $\rho = 7850$  kg / m<sup>3</sup>. The material properties of the cutter head are as follows: elastic modulus  $E = 520$  GPa, poisson's ratio  $\nu = 0.22$ , and density  $\rho = 12,000$  kg / m<sup>3</sup>.

#### B. Finite element mesh generation

In ANSYS, meshing can be said to be a crucial step. because the quality of meshing directly affects the accuracy and speed of solution, we often need to modify the meshing. meshing is a very practical modification method. The grid division of the blade is refined in the cutter head part. The tooth part of the worm is also refined.

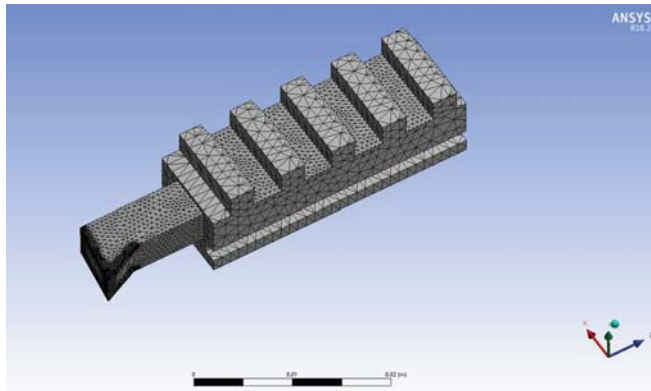


Fig. 6. Ansys mesh division of cutting head

The main purpose of finite element analysis is to check the structural response to certain load conditions. Therefore, it is also a key step to specify suitable load conditions in the analysis. Proper loading will be able to better simulate the actual situation and correctly reflect the mechanical characteristics of the actual structure.

#### C. Results

It can be seen from the above stress and displacement distribution map that the maximum stress and strain experienced by the cutter head appear at the position of the cutting edge. The maximum deformation of the cutter head is 0.2mm and the maximum stress is  $2.8 \times 10^9$ Pa..

At the same time, some relevant analysis is also carried out on the turbine. Based on SolidWorks solid model of large gear, the material is set as alloy steel. The load is applied to the tooth profile surface of the worm wheel in the form of normal force, wherein the normal force direction is perpendicular to the tooth profile surface and the normal force is uniform load of 100 n.. An axial constraint and a radial constraint are applied to the outer surface of the protruding shaft of the worm wheel. The solid model of the worm wheel

is meshed by finite element method and the displacement diagram of the worm wheel is obtained by simulation calculation as shown in figure 66, and the worm wheel should try to be as shown in figure 67. The deformation result of the worm wheel in the figure is enlarged 36033 times in proportion. Analysis of the data in fig. 4.3 and fig. 4.4 shows that the maximum deformation of the worm wheel is 0.00038 mm and the maximum stress is 10.97 MPa .

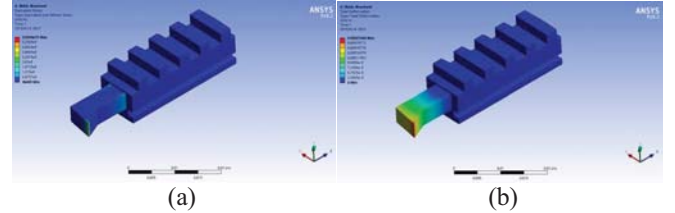


Fig. 7. Deformation diagram(a) and stress diagram of cutter head (b)

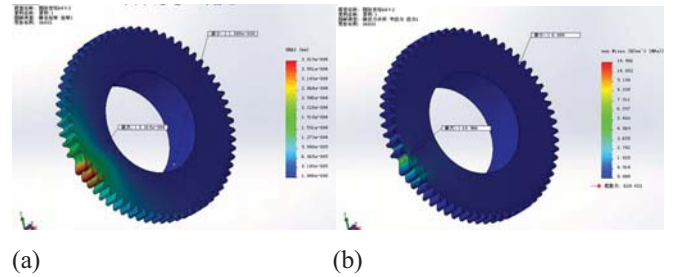


Fig. 8. The overall appearance of the high pressure cutting device

#### IV. RESULTS AND DISCUSSION

This previous version of the cutting device was designed to cut gas hydrate sampling tubes acquired in shenhu sea, south China sea. Good results have been obtained in practical operation.



Fig. 9. The previous version of the cutting device



Fig. 10. Test piece for cutting mechanism

This high pressure pressure cutting device has not been made into real material, which is used for the actual gas hydrate sampling pipe cutting. We believe that with this design, better cutting effects will be presented.

## V. CONCLUSION

Compared with the existing technology, the beneficial effect of the invention is:

- A. The cutting device has pressure balance at the same time of resisting high pressure, and avoids installation difficulty caused by different internal and external pressure.
- B. The structure is simple, the structure is basically symmetrical, and the installation is convenient and simple.
- C. The cutting is uniform, the disturbance of the cutting process to the sample is reduced, the sample cutting device does not generate secondary pollution to the sample, and the cutting is carried out under the conditions of pressure maintaining and temperature control.
- D. The cutting process is controllable, and the cutting depth can be accurately controlled according to the lead of the Archimedes spiral line.
- E. By adjusting the speed of the motor, the cutting and cutting speed and cutting speed can be controlled, both high cutting speed and low feed speed can be met at the same time, and the cutting speed can be fast when needed.
- F. By adjusting the speed and rotation direction of the clamping motor, we can clamp and release the sample tube, and also control the clamping and loosening speed.

The difficulty lies in the design and control of the cutter head and jaw. The cutter head must be fed at the same time and the sampling tube must be cut at the same time.

Requirements for the concentricity of the spiral groove disc and the limit disc are put forward. The cutter head needs to be able to be retracted repeatedly so as not to affect the movement of the sampling tube inside the cutting device and at the same time to reach the center of the circle of the sampling tube.

The cutting device will be processed in the following period of time, and there is reason to believe that better cutting effect will be shown.

## ACKNOWLEDGMENT

Thanks to Mr. Jiawang Chen for his guidance and financial support, I have proposed some revisions to my immature ideas and helped me to contact mechanical engineers during the design process. Providing manufacturers in the processing chain has given me the opportunity to put into practice. Thanks to Lin Yuan's mentor for my simulation and for answering my simulation questions. Thanks to the help of our classmates and teachers, it is hard to forget the days of discussion together.

## REFERENCES

- [1] Jie Dong, research on residual stress of high speed steel turning tool quenching and cryogenic treatment, 2014, Zhejiang university. p. 61.
- [2] Jiawang Chen et al, pressure maintaining system of pressure maintaining transfer device for natural gas hydrate. journal of marine technology, 2017 ( 02 ): 23 - 27.
- [3] Jiawang Chen et al, study on pressure characteristics of gas hydrate pressure maintaining subsampler. ocean engineering, 2017 ( 05 ): pp. 103 - 109.
- [4] Gang Zhan et al, finite element simulation of residual stress of cemented carbide micro-pit turning tool for 304 stainless steel cutting. combined machine tool and automated processing technology, 2017 ( 08 ): pp. 37 - 39.